

Learn from Heterophily: Heterophilous Information-enhanced Graph Neural Network

Yilun Zheng¹, Jiahao Xu¹, and Lihui Chen¹ (✉)

Centre for Info. Sciences and Systems,
Nanyang Technological University, Singapore
yilun001@e.ntu.edu.sg, jiahao004@e.ntu.edu.sg, elhchen@ntu.edu.sg

Abstract. Under circumstances of heterophily, where nodes with different labels tend to be connected based on semantic meanings, Graph Neural Networks (GNNs) often exhibit suboptimal performance. Current studies on graph heterophily mainly focus on aggregation calibration or neighbor extension and address the heterophily issue by utilizing node features or structural information to improve GNN representations. In this paper, we propose and demonstrate that the valuable semantic information inherent in heterophily can be utilized effectively in graph learning by investigating the distribution of neighbors for each individual node within the graph. The theoretical analysis is carried out to demonstrate the efficacy of the idea in enhancing graph learning. Based on this analysis, we propose HiGNN, an innovative approach that constructs an additional new graph structure, that integrates heterophilous information by leveraging node distribution to enhance connectivity between nodes that share similar semantic characteristics. We conduct empirical assessments on node classification tasks using both homophilous and heterophilous benchmark datasets and compare HiGNN to popular GNN baselines and SoTA methods, confirming the effectiveness in improving graph representations. In addition, by incorporating heterophilous information, we demonstrate a notable enhancement in existing GNN-based approaches, and the homophily degree across real-world datasets, thus affirming the efficacy of our approach.

Keywords: Graph Neural Networks · Graph Homophily · Heterophilous Information.

1 Introduction

Graph-structured data widely exists in various applications including social networks [8] and recommendation systems [21] where entities are connected by their relations. To learn representations from these relational graphs, Graph Neural Networks (GNNs) [9, 10, 17] are proposed and have made substantial advancements. The effectiveness of GNNs on graph-structured data largely hinges on the homophily assumption, which posits that connected nodes tend to be similar [25]. Under this assumption, information is aggregated from neighboring nodes with similar features, facilitating effective information exchange within

local structures. However, the homophily assumption does not always hold in many real-world scenarios where dissimilar nodes are connected [26], a situation referred to as heterophily or non-homophily. Heterophily poses a limitation to the performance of GNNs as it involves the aggregation of information from dissimilar nodes, thereby introducing additional noise during the aggregation process.

To tackle the heterophily issue in graphs, several approaches have been proposed. Some methods calibrate the aggregation process by integrating high-order neighbors with different weights [1, 4, 18, 28], introducing adjacency matrices as a new feature of nodes [12], or propagating prior belief estimations [27]. While these aggregation calibration methods have demonstrated some improvements on heterophily graphs, they primarily focus on local neighbors and fail to aggregate information from global neighbors. Consequently, alternative methods are proposed to aggregate signals from global neighbors by integrating new filters [2, 13], or construct new graph structures [11, 14, 16, 23].

Despite the demonstrated effectiveness of these methods for heterophilous graphs, they overlook the information of heterophily during graph representation learning process, resulting in a suboptimal problem. Existing methods characterize the node information in graphs using features, structures, or aggregated neighbor features, yet none of them explain how nodes become homophilous or heterophilous.

In this paper, we measure the heterophilous information as neighbor distribution, which describes the probability of a node’s neighbors belonging to specific classes. This information not only provides insight into the degree of homophily or heterophily but also enhances our understanding of the heterophilous contexts of nodes. We conduct both theoretical and empirical analyses to assess the impact of heterophilous information on graph learning. The results show that heterophilous information is effective in identifying semantically similar nodes. Building upon this analysis, we propose a novel method, **HiGNN** (**H**eterophilous **I**nformation-enhanced **G**raph **N**eural **N**etwork), designed to incorporate heterophilous information into GNNs. Leveraging this heterophilous information, the HiGNN demonstrates superior performance on both the homophilous and heterophilous datasets, significantly improving the homophily degree within newly constructed graph structures. In summary, our main contributions are summarized as follows:

- We first define the conception of heterophilous information in graphs and validate the effectiveness in improving homophily through both theoretical and empirical analysis.
- We propose HiGNN, a novel method that leverages heterophilous information in GNNs. By constructing a new adjacency matrix based on the similarity of heterophilous information, HiGNN establishes new connections for nodes with similar heterophilous semantics, resulting in an improved homophily degree across different levels of homophily.

- Our experimental results demonstrate the superiority of our method on both the homophilous and heterophilous datasets. We also show improvements over general GNN baselines by incorporating heterophilous information.

2 Background

We denote $\mathcal{G} = (\mathcal{V}, \mathcal{E})$ as an undirected graph \mathcal{G} with node set \mathcal{V} and edge set \mathcal{E} . Let A be an adjacency matrix where $A_{ij} = 1$ or $A_{ij} = 0$ represents the presence or absence of an edge e_{ij} connecting node v_i and v_j . For each node v_i , we use $\mathcal{N}_i = \{v_j | A_{ij} = 1\}$ to denote its 1-hop neighbor set and d_i to denote its node degree. We represent the node features as $X = \{x_1, x_2, \dots, x_n\} \in \mathbb{R}^{N \times M}$ and the labels as $Y = \{y_1, y_2, \dots, y_n\} \in \mathbb{R}^{N \times 1}$.

Graph Neural Networks (GNNs) are a class of neural networks designed to process graph-structured data. Based on the message passing mechanism, GNNs enable nodes to exchange information with their neighbors. In the l -th layer of GNN, the representation z_i for node v_i is updated as follows:

$$z_i^l = \text{UPDATE}^l \left(z_i^{l-1}, \text{AGGREGATE}^l(z_i^{l-1}, \{z_j^{l-1} | v_j \in \mathcal{N}_i\}) \right) \quad (1)$$

where $\text{AGGREGATE}(\cdot)$ describes the aggregation of information from node v_i and its neighbors \mathcal{N}_i , and $\text{UPDATE}(\cdot)$ describes how the representation z_i^l is updated based on ego representation z_i^{l-1} and aggregated neighbor representations. The Graph Convolutional Network (GCN) is one of the representative of GNNs and the output of its l -th layer can be represented as:

$$Z^l = \sigma(\hat{A}Z^{l-1}W^{l-1}) \quad (2)$$

Here an activation function σ is applied to the normalized adjacency matrix $\hat{A} = \tilde{D}^{-\frac{1}{2}} \tilde{A} \tilde{D}^{-\frac{1}{2}}$, where $\tilde{D} = D + I_n$ and $\tilde{A} = A + I_n$ represent the degree matrix and adjacency matrix with added self-loops.

Graph homophily is the fundamental assumption of GNNs, where similar nodes are likely to be connected. This principle of homophily enhances the efficacy of information propagation within GNNs, as it aggregates the representations of nodes sharing identical labels. The commonly used metrics for graph homophily include edge homophily [1] and node homophily [15], which can be defined as:

$$h_{edge} = \frac{|\{e_{ij} | e_{ij} \in \mathcal{E}, y_i = y_j\}|}{|\mathcal{E}|}, h_{node} = \frac{1}{|\mathcal{V}|} \sum_{v_i \in \mathcal{V}} \frac{|\{v_j | v_j \in \mathcal{N}_i, y_i = y_j\}|}{d_i} \quad (3)$$

where the edge homophily h_{edge} represents the ratio of homophilous edges in the entire graph and the node homophily h_{node} calculates the average homophily degree across all nodes. Since h_{edge} and h_{node} show little difference in the datasets used in this paper, we only consider and discuss edge homophily, denoted as h , in the following section.

3 Methodology

In this section, we first introduce the definition of heterophilous information in Sect. 3.1. Next, we analyze how heterophilous information improves graph learning in Sect. 3.2. Finally, we introduce our proposed method HiGNN in Sect. 3.3.

3.1 Heterophilous Information

In heterophilous graphs, nodes with different labels tend to be connected. Consequently, many studies [11, 16, 27] perceive heterophily as a challenge in graph representation learning and propose methods to address the heterophily by utilizing node features or structural information. During the process, however, the heterophilous information, which could be helpful for graph representation learning, is discarded. Next, we give the definition of heterophilous information and discuss its benefits in improving graph learning.

Definition 1. *For any node u in the graph \mathcal{G} , the heterophilous information \mathcal{H} is defined as its neighbor distribution, which describes how nodes become heterophilous:*

$$\mathcal{H}_u = [p_1, p_2, \dots, p_c], \text{ where } p_i = \frac{|\{v | v \in \mathcal{N}_u, y_v = i\}|}{|\mathcal{N}_u|} \quad (4)$$

Here each element p_i at position i in \mathcal{H}_u describes the probability of node neighbors \mathcal{N}_u belongs to class i . Compared with the definition of node homophily in Eq. (3), heterophilous information better characterizes the heterophilous context of a node: for any node u with class i , when its homophily is very high e.g. $h \rightarrow 0$, the \mathcal{H}_u is approximate to an all-zero vector with $p_i \rightarrow 1$. On the contrary, low homophily results in the $p_i \rightarrow 0$ in \mathcal{H}_u . In this case, the other entries of \mathcal{H}_u describe how the node becomes heterophilous, while h , a single scalar value, is insufficient to describe the heterophilous contexts of a node.

Next, to utilize the heterophilous information, we create a new adjacency matrix A' by connecting the nodes that share a high similarity of \mathcal{H} , where Each entry $A'_{i,j}$ can be expressed as

$$A'_{i,j} = \mathbb{1}(\cos(\mathcal{H}_i, \mathcal{H}_j) > \delta) \quad (5)$$

where $\mathbb{1}$ is an indicator function that is equal to 1 when the cosine similarity of heterophilous information of nodes i and j larger than a threshold δ , otherwise, it is equal to 0.

3.2 Analysis of Heterophilous Information

After defining the new adjacency matrix A' with heterophilous information, we analyze how well this approach improves graph learning under general circumstances. Therefore, we assume each entry of \mathcal{H} is corrupted by a Gaussian noise

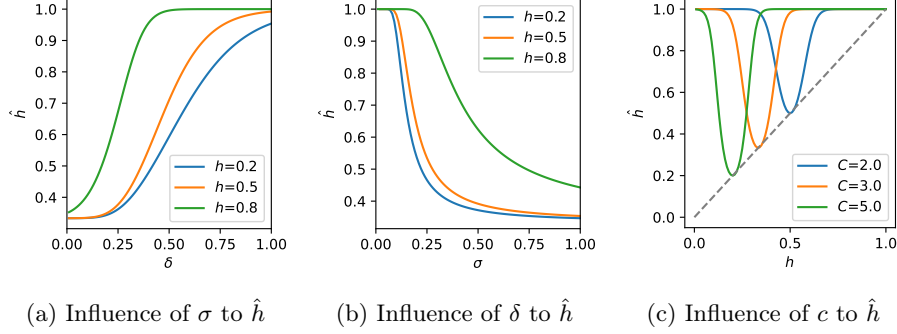


Fig. 1: Relation of improved homophily and original homophily under different parameter setting. Fig. (a), (b), and (c) shows the relation under different δ , σ , and c respectively.

$\epsilon \sim N(0, \sigma^2)$. Then we analyze the performance of graph learning with A' by theoretically examining the homophily degree \hat{h} of A' (proofs in Appendix A).

Theorem 1. *The homophily degree \hat{h} of A' is directly proportional to the threshold δ , inversely proportional to the variance σ^2 of sampling noise, and directly proportional to the distance between the original homophily degree and reciprocal of c :*

$$\hat{h} \propto \delta, \hat{h} \propto \frac{1}{\sigma^2}, \hat{h} \propto |h - \frac{1}{c}| \quad (6)$$

To better illustrate the relationships, we plot the influences of these parameters. As depicted in Fig. 1a and Fig. 1b, \hat{h} is directly proportional to δ and inversely proportional to σ under different levels of h . These results align with our intuition: a larger noise during neighbor sampling makes it more challenging to capture their true neighbor distribution, thereby reducing \hat{h} . Moreover, a higher δ allows fewer edges with a higher similarity of neighbor distribution to connect, thereby increasing \hat{h} . Regarding the influence of h , as shown in Fig. 1c, an larger distance between h and $\frac{1}{c}$ improves \hat{h} . When $h = \frac{1}{c}$, the probability of edges connecting to intra-class or inter-class nodes becomes identical i.e. $P(\mathbf{S}^+ > \delta) = P(\mathbf{S}^- > \delta)$, which implies that there is no useful information from neighbors with respect to class. Conversely, if h is very high or low, the neighbor distribution becomes distinguishable for each class, leading to an improved \hat{h} .

We then measure the influences of these parameters on real-world datasets. As depicted in Table 1, we measure the average standard deviation $\bar{\sigma}$, original homophily h , and the homophily improvement $\hat{h} - h$ under different threshold δ across 6 datasets. The results of $\hat{h} - h$ are shown in blue color if there is a positive improvement. The results align with our theoretical analysis: a larger δ improves \hat{h} while a larger $\bar{\sigma}$ decreases \hat{h} . It is worth noting that the $\bar{\sigma}$ is typically

small, resulting in a large improvement in \hat{h} as shown in 1a. This shows the newly constructed A' effectively improves the graph learning. This is further evidenced in Table 1 where most datasets exhibit a significant increase of homophily with a high σ .

Table 1: Homophily Improvement on Heterophilous Datasets

Dataset	Texas	Squirrel	Wisconsin	Chameleon	Cornell	Actor
$\bar{\sigma}$	0.2328	0.2623	0.2837	0.2752	0.2471	0.3122
h	0.0609	0.1778	0.2960	0.2299	0.2221	0.2167
$\hat{h} - h, \delta = 0.3$	0.4189	0.1768	0.0863	-0.0133	-0.0233	-0.0034
$\hat{h} - h, \delta = 0.6$	0.4634	0.2357	0.0940	-0.0005	-0.0206	-0.0037
$\hat{h} - h, \delta = 0.8$	0.4827	0.3399	0.0951	0.0212	-0.0142	-0.0037
$\hat{h} - h, \delta = 0.9$	0.5404	0.4238	0.0865	0.0605	-0.0051	-0.0040
$\hat{h} - h, \delta = 1.0$	0.6447	0.5152	0.1129	0.2448	0.1743	-0.0030

3.3 HiGNN

In this subsection, we present our method, Heterophilous Information-enhanced Graph Neural Networks(HiGNN), which is based on the preceding analysis of heterophilous information.

Graph structure construction. Figure. 2 illustrates the process of the construction of a new adjacency matrix A' by incorporating heterophilous information \mathcal{H} . As shown on the left side, we first obtain all the labels Y' . Here we follow the conventional setting of graph-based semi-supervised learning [6, 7] to estimate the labels A' of all nodes by training an off-the-shelf model on the training data X_{train} and Y_{train} :

$$\min_{\mathcal{M}} \mathcal{L}(\mathcal{M}(X_{train}), Y_{train}), Y' = \mathcal{M}(X) \quad (7)$$

where $\mathcal{M}(\cdot)$ represents an off-the-shelf model and \mathcal{L} denotes its loss function. After obtaining all the estimated labels Y' , we derive the heterophilous information \mathcal{H} of all nodes by their neighbor distribution using Eq. (4). Finally, based on \mathcal{H} , we construct A' by preserving connections with high similarity of \mathcal{H} using Eq. (5).

For the nodes exhibiting high homophily or heterophily, denoted as red nodes or yellow nodes respectively in Fig. 2, our method effectively groups them within the same class. Additionally, our method can also connect nodes with half-homophily, represented by a dashed stroke in Fig. 2. These half-homophily nodes, which act as boundary nodes straddling two classes, share similar semantics. While connecting boundary nodes with nodes inside the class boundary increases homophily, it may have detrimental effects on graph learning. This

is due to the influence of connections with other types of nodes on boundary nodes, leading to different patterns that manifest as mediators. Our new adjacency matrix establishes connections among boundary nodes and facilitates message passing among nodes with similar semantics, thereby contributing to effective graph learning at various homophily levels.

Although this label estimation is not flawless and may result in a biased estimation of heterophilous information \mathcal{H} , the \mathcal{H} defined in this paper is error-tolerant, accommodating differences between neighbor distributions in similar nodes. As illustrated in 1a, for δ that is close to 1, the improved homophily \hat{h} does not decrease significantly. Our experimental analysis of homophily improvement across 9 real-world datasets in Fig. 3 further substantiates this proposition.

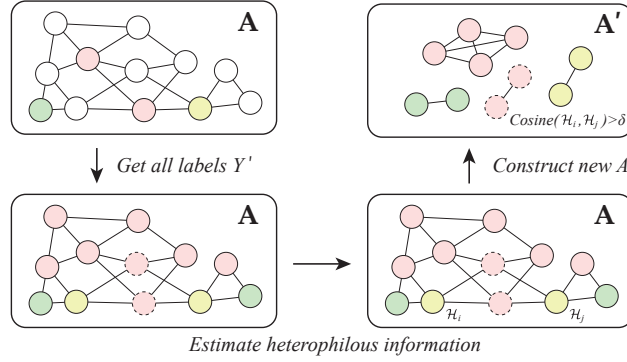


Fig. 2: The construction process of new adjacency matrix A' with heterophilous information. We first obtain all labels Y' by training an off-the-shelf model on the training data. Then based on the estimated labels, we measure the heterophilous information \mathcal{H} on all the nodes. Finally, nodes with similar \mathcal{H} are connected in the A' .

Channel Fusion. Although the newly constructed adjacency matrix A' contains rich heterophilous information with improved homophily degree, the original adjacency matrix A is informative as well. To retain the original graph topological information as a supplement, we employ a late fusion strategy on these two graph topologies. Specifically, for the node embeddings Z_{l-1} at layer $l-1$, we perform graph convolution on A' and A to obtain the updated node embeddings of the next layer Z_{new}^l and Z_{old}^l respectively,

$$Z_{new}^l = g(\hat{A}' Z^{l-1} W^{l-1}), Z_{old}^l = g(\hat{A} Z^{l-1} W^{l-1}) \quad (8)$$

where \hat{A}' and \hat{A} denote the normalized adjacency matrices of A' and A respectively, $g(\cdot)$ is an activation function, and W^{l-1} is a weight matrix. Given that the heterophilous information is a new addition and its contribution to the final result could vary depending on specific datasets, we introduce a balance param-

eter λ for the late fusion of the embeddings from two channels, which could be expressed as:

$$Z^l = \lambda Z_{new}^l + Z_{old}^l \quad (9)$$

The balance parameter λ is used to regulate the proportion of heterophilous information incorporated in the learning process. A higher λ emphasizes heterophilous information, while a lower λ emphasizes original topological information. The choice of late fusion, as opposed to combining the two adjacency matrices early, was deliberately taken to keep the heterophilous and topological information unperturbed from each other. This approach ensures that the unique contributions of each can be captured separately, allowing each to fully express the nuances of its information channels.

3.4 Complexity Analysis

The time complexity of HiGNN mainly comes from three parts: (1) label estimation with GNNs $\mathcal{O}(L|\mathcal{V}|MF + L|\mathcal{E}|F)$, (2) heterophilous information collection $\mathcal{O}(|\mathcal{E}|)$, (3) new adjacency matrix construction $\mathcal{O}(c|\mathcal{V}|^2)$, and (4) graph convolution on two channels $\mathcal{O}(2L|\mathcal{V}|MF + 2L|\mathcal{E}|F)$, where L , M , F , and c refer to the number of graph convolution layers, node feature dimension, hidden embedding size, and class number respectively. The complexity of graph convolution is linear to the general GNNs baselines and the total complexity of constructing new adjacency matrix A' with heterophilous information is $\mathcal{O}(L|\mathcal{V}|MF + L|\mathcal{E}|F + |\mathcal{E}| + c|\mathcal{V}|^2)$, which is comparable to the other neighbor extension methods.

4 Experiments

4.1 Experimental Setup

Baselines. We benchmark HiGNN against a variety of methods, including non-graph methods, general GNNs, and heterophily-oriented GNNs. Specifically, we use MLP as the graph-agnostic method and GCN [10], GAT [17], SGC [19], Mix-hop [1], and GraphSage [9] as the general GNNs baselines. For the heterophily-oriented GNNs, we use GCN2 [3], H2GCN [28], LINKX [12], ACMGCN [13], and GPRGNN [4], GloGNN [11], WRGAT [16], and GGCN [23].

Datasets. We measure all the methods on 3 homophilous datasets¹ and 6 heterophilous graph datasets². The statistics of all the datasets are presented in Table 2, where the homophilous graphs including Cora, CiteSeer, and PubMed, exhibit a significantly higher homophily compared to heterophilous graphs. We run 10 times for each dataset following public random splits with the ratio of 60%/20%/20% for train, validation, and test sets respectively³.

¹ <https://github.com/kimiyoung/planetoid/tree/master/data>

² <https://github.com/CUAI/Non-Homophily-Large-Scale/tree/master/data>

³ <https://github.com/bingzhewei/geom-gcn/tree/master/splits>

Table 2: Dataset Statistics

Dataset	Cora	CiteSeer	PubMed	Chameleon	Cornell	Actor	Squirrel	Texas	Wisconsin
#Nodes	2,708	3,327	19,717	2,277	183	7,600	5,201	183	251
#Edges	10,556	9,104	88,648	38,328	478	37,526	222,134	492	750
#Features	1,433	3,703	500	2,325	1,703	932	2,089	1,703	1,703
#Classes	7	6	3	5	5	5	5	5	5
h_{edge}	0.81	0.74	0.80	0.23	0.30	0.22	0.22	0.06	0.17
h_{node}	0.83	0.72	0.79	0.25	0.39	0.22	0.22	0.10	0.15

Implementations. To generate label predictions for neighbor distribution, we select ACM-GCN as an off-the-shelf model. Given the flexibility of our method, which can be integrated into any GNN method, we adopt GCN as the backbone model, enhanced with a high-pass filter [13]. Then we run HiGNN and all the baselines on 9 datasets, implemented using Pytorch on an A5000 GPU. The models are trained until convergence is achieved, with an early stopping criterion of 40 epochs or a maximum of 2000 epochs. For all the baselines, we search for the optimal hyper-parameters, including hidden embedding size, learning rate, weight decay, and dropout rate on the validation sets. Specifically for HiGNN, we search for the threshold δ from $[0.5, 0.8, 0.9, 1.0]$ and lambda λ from $[1, 0.5, 0.1, 0.05, 0.01]$ for each dataset.

4.2 Performance

Table 3 shows a comparison of HiGNN with other baselines. All methods are evaluated with node classification task, where both the mean accuracy and standard deviation are reported based on 10 public random splits. The average rank for each method is calculated across 9 datasets, with a lower rank indicating better performance. For each dataset, the best-performing methods are highlighted in **bold** and the runner-up methods are underlined. For methods that augment general GNN baselines with heterophilous information (denoted as +Hi), we halve the embedding space to control the total number of parameters and time complexity, ensuring a fair comparison. If there is an improvement over the original methods, the results are displayed in [blue](#).

First, our proposed HiGNN generally outperforms all the other methods, achieving the lowest average rank, indicating the effectiveness of incorporating heterophilous information into graph learning. HiGNN enhances the performance on both the homophilous and heterophilous datasets, corroborating the explanation provided in Sect. 3.2 that the new matrix constructed by heterophilous information improves graph learning at different homophily levels. Besides, the effectiveness of heterophilous information is also shown in the improvement on the general GNNs baselines where the performances are improved on most of the datasets. Second, compared with general GNN baselines such as GCN and GAT, MLP performs poorly on homophilous graphs but still demonstrates strong performance on heterophilous graphs. This validates the asser-

tion that heterophily impedes graph convolution in graph learning. Then for the methods that aggregate embeddings of k-hop neighbors during the message passing, Mixhop, H2GCN, GGCN, CPGCN, and GPR-GNN show their improvement with respect to GCN, but they still have a large gap with HiGNN and GloGNN that exploit global similar nodes. This indicates that for heterophilous graphs, focusing on k-hop neighbors is not as sufficient as constructing new graph structures that capture neighbors with similar semantics. Note that although GloGNN delivers the best results on 3 datasets, it requires the calibrated adjustment of many parameters. In contrast, our method is more straightforward and flexible, requiring fewer parameter tunings.

Table 3: Node classification performance of HiGNN

Methods	Cora	CiteSeer	PubMed	Chameleon	Cornell	Actor	Squirrel	Texas	Wisconsin	Rank↓
GCN	86.90 ± 1.09	75.33 ± 2.07	87.85 ± 0.37	49.21 ± 2.56	63.24 ± 6.40	31.08 ± 0.65	26.57 ± 1.47	57.57 ± 4.24	57.65 ± 5.33	15.17
GCN+Hi	87.04 ± 1.24	75.73 ± 2.26	88.40 ± 0.57	61.18 ± 2.51	65.95 ± 6.00	31.74 ± 0.97	28.99 ± 3.44	60.00 ± 3.99	59.61 ± 7.58	12.44
GAT	86.06 ± 1.31	74.65 ± 1.26	86.75 ± 0.58	68.46 ± 1.99	56.22 ± 5.06	27.84 ± 1.46	60.46 ± 2.18	57.57 ± 8.92	54.90 ± 6.85	13.72
GAT+Hi	86.78 ± 1.80	75.32 ± 1.63	87.08 ± 0.47	68.49 ± 1.66	58.38 ± 4.80	28.14 ± 1.12	61.37 ± 2.10	57.03 ± 7.59	58.04 ± 6.87	11.89
GraphSage	80.44 ± 1.90	74.53 ± 1.62	86.54 ± 0.48	51.34 ± 2.02	74.59 ± 5.58	34.12 ± 1.79	31.55 ± 2.26	70.81 ± 9.35	79.41 ± 3.61	13.22
GraphSage+Hi	80.78 ± 2.03	74.98 ± 1.21	87.14 ± 0.47	52.43 ± 2.34	73.24 ± 6.17	34.03 ± 1.17	32.05 ± 1.79	70.27 ± 8.73	80.20 ± 3.97	12.11
SGC	84.97 ± 1.95	75.66 ± 1.37	87.15 ± 0.47	64.78 ± 1.98	55.41 ± 5.29	25.83 ± 1.09	41.78 ± 2.88	58.11 ± 6.27	57.84 ± 4.83	14.11
SGC+Hi	85.25 ± 1.58	76.13 ± 2.26	88.84 ± 0.73	61.86 ± 2.92	71.89 ± 6.27	34.17 ± 0.95	41.98 ± 1.16	64.05 ± 7.21	73.53 ± 5.79	10.00
Mixhop	86.58 ± 1.12	75.14 ± 1.62	88.53 ± 0.48	62.35 ± 1.48	65.14 ± 6.91	31.76 ± 2.06	40.16 ± 5.78	60.81 ± 6.40	66.86 ± 5.18	12.33
Mixhop+Hi	87.20 ± 0.96	75.72 ± 1.59	88.90 ± 0.55	63.31 ± 2.47	66.22 ± 3.87	33.70 ± 1.26	42.47 ± 2.19	62.70 ± 6.22	69.02 ± 5.76	9.67
MLP	74.25 ± 2.16	72.09 ± 1.34	87.07 ± 0.30	49.87 ± 2.41	77.57 ± 7.43	35.65 ± 0.66	32.80 ± 1.43	76.22 ± 8.24	81.76 ± 4.98	11.61
ACM-GCN	87.83 ± 0.95	75.56 ± 1.32	89.48 ± 0.58	67.94 ± 1.68	77.57 ± 5.26	35.09 ± 1.18	53.35 ± 1.33	82.70 ± 6.27	83.53 ± 3.83	4.39
GCN2	86.80 ± 1.08	74.84 ± 1.48	88.27 ± 0.72	65.07 ± 2.71	54.32 ± 9.14	33.48 ± 2.05	52.68 ± 0.98	61.89 ± 6.43	56.86 ± 8.32	12.56
H2GCN	87.71 ± 1.25	76.32 ± 1.54	89.17 ± 0.45	65.88 ± 2.38	75.95 ± 7.37	36.23 ± 0.98	57.08 ± 1.58	75.68 ± 6.74	80.59 ± 2.99	4.78
GPR-GNN	87.42 ± 1.21	75.43 ± 1.47	89.18 ± 0.51	67.17 ± 1.47	74.32 ± 3.66	35.47 ± 1.66	43.84 ± 3.07	74.86 ± 5.70	79.61 ± 5.56	6.78
WRGAT	75.47 ± 2.90	74.14 ± 1.40	OOM	51.40 ± 2.24	76.49 ± 6.75	36.15 ± 1.00	30.73 ± 1.70	76.76 ± 4.07	79.61 ± 5.16	12.22
GGCN	86.32 ± 0.91	76.65 ± 1.91	88.25 ± 0.43	56.49 ± 2.65	71.35 ± 7.34	34.86 ± 0.87	39.18 ± 1.87	65.14 ± 8.30	74.12 ± 5.37	10.33
LINKX	77.32 ± 1.68	72.00 ± 1.90	78.39 ± 1.09	68.38 ± 2.50	39.46 ± 17.89	27.06 ± 1.22	59.15 ± 2.06	52.43 ± 9.21	55.88 ± 6.29	15.78
GloGNN	88.31 ± 1.15	77.41 ± 1.65	89.62 ± 0.35	65.59 ± 2.21	82.16 ± 5.82	37.36 ± 1.34	29.44 ± 1.36	69.19 ± 11.16	82.35 ± 5.11	5.00
HiGNN	89.72 ± 1.46	79.30 ± 2.13	89.43 ± 0.53	68.86 ± 1.45	80.00 ± 4.26	37.21 ± 1.35	54.78 ± 1.58	86.22 ± 4.67	85.88 ± 3.18	1.89

4.3 Improvement in Homophily Degree

To validate that the new graph structure A' with heterophilous information in HiGNN improves homophily, we measure the homophily degree for both the original graph structure A and the new graph structure A' . Specifically, we compute homophily degrees across 9 datasets on 10 random splits and then report the mean and standard deviation. As depicted in Fig. 3, the newly constructed matrix improves the homophily degree on all datasets, particularly for heterophilous datasets. This suggests that heterophilous information is helpful in grouping semantically similar nodes. It is worth noting that the estimation of heterophilous information is based on the predicted labels instead of the true labels, demonstrating the estimation is error-tolerant as suggested in Sect. 3.3

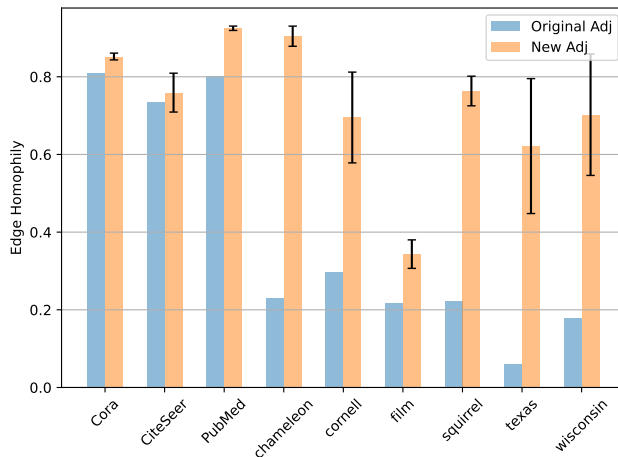


Fig. 3: The homophily improvement after constructing new adjacency matrices with heterophilous information. For each dataset, we show the mean and standard deviation of the newly constructed matrix based on 10 splits.

4.4 Ablation Study

To demonstrate the performance improvement of HiGNN achieved through the incorporation of heterophilous information and the efficacy of the fusion strategy employed in HiGNN, we undertake an ablation study. As shown in Table 4, for HiGNN, we examine the influence of channels by removing the new channel (w/o A'), removing the original channel (w/o A), or fusing two adjacency matrices A and A' in one channel ($A+A'$). The results show that the performance of HiGNN drops when either the new channel or the original channel is removed. This suggests that optimal performance is attained by considering different aspects of these two channels. Furthermore, the early fusion of two adjacency matrices ($A+A'$) underperforms compared to the late fusion in HiGNN, indicating the late fusion strategy allows the model to fully capture the unique contributions of each channel as suggested in Sect. 3.3.

Table 4: Ablation study on HiGNN

Methods	Cora	CiteSeer	PubMed	Chameleon	Cornell	Actor	Squirrel	Texas	Wisconsin	Rank↓
HiGNN	89.72 ± 1.46	79.30 ± 2.13	89.43 ± 0.53	68.86 ± 1.45	80.00 ± 4.26	37.21 ± 1.35	54.78 ± 1.58	86.22 ± 4.67	85.88 ± 3.18	1.56
w/o A'	87.83 ± 0.95	75.56 ± 1.32	89.48 ± 0.58	67.94 ± 1.68	77.57 ± 5.26	35.09 ± 1.18	53.35 ± 1.33	82.70 ± 6.27	83.53 ± 3.83	3.78
w/o A	87.63 ± 1.29	75.20 ± 1.79	88.15 ± 0.65	63.86 ± 1.42	75.41 ± 5.76	33.98 ± 1.20	46.68 ± 1.32	76.49 ± 5.56	82.75 ± 4.87	8.00
$A + A'$	87.40 ± 1.34	75.31 ± 1.93	88.04 ± 0.64	68.00 ± 1.87	78.11 ± 5.17	34.03 ± 1.25	54.18 ± 1.33	81.89 ± 4.60	83.53 ± 5.16	5.06

4.5 Hyper-parameter Analysis

This section introduces the influence of the threshold parameter δ and the lambda parameter λ on HiGNN. The δ modulates the similarity threshold of heterophilous information in constructing A' and the λ balances the significance of the new channel within the HiGNN framework. As shown in Fig. 4a a smaller λ leads to a decrease in model performance for both datasets, indicating the necessity of introducing heterophilous information. An overlarge λ also leads to the degradation of the performance, especially for Chameleon. This implies the optimal λ should be selected from 0.1 to 1. For the threshold δ as shown in Fig. 4b, the performance of HiGNN becomes better with the increase of δ . This shows a larger δ could capture more efficient connections between semantically similar nodes, which correlates with the Theorem 2.

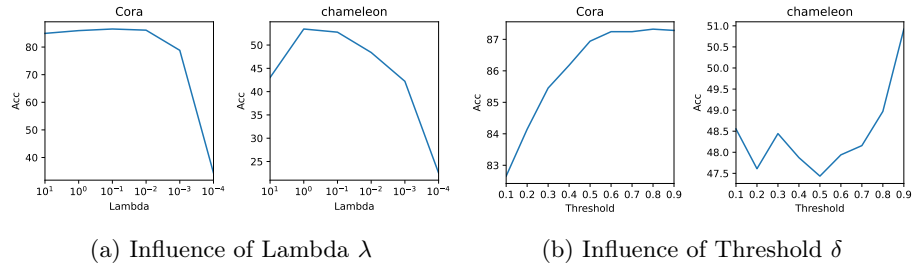


Fig. 4: The hyper-parameter analysis of lambda λ and threshold δ in HiGNN on homophilous dataset(Cora) and heterophilous dataset(Chameleon)

5 Related Work

5.1 Graph Neural Networks

Graph Neural Networks are effective for handling graph-structured data [5, 24]. These networks capture the dependencies between nodes through a message-passing mechanism. As a representative of GNNs, Graph Convolutional Networks (GCNs) [10] performs convolution on the spectral domain to aggregate information from neighbors, capturing the relationships between nodes in graphs. Graph Attention Networks (GATs) [17] specify different weights to different neighbors with attention mechanisms, enabling the model to focus on the most important information. For inductive representation learning, GraphSage [9] generates low-dimensional vectors by learning a function that aggregates neighbors. These GNNs operate effectively under the assumption of homophily, which posits that connected nodes tend to exhibit similarity. However, these methods experience significant performance degradation in heterophilous graphs, where connected nodes are more likely to have different labels. [25].

5.2 Graph Homophily

To solve the issue of graph heterophily, many methods have been proposed to improve graph representation learning. These methods can be categorized into two classes: aggregation calibration methods and neighbor extension methods.

The aggregation calibration methods primarily focus on improving message aggregation. Mixhop [1] integrates embeddings of k -hop neighbors during the graph convolution and employs trainable aggregation parameters for each hop. Following these high-order aggregations of neighbors, H2GCN [28] further distinguishes between ego and neighbor embeddings and combines intermediate representations with theoretical justification. GPR-GNN [4] uses a Generalized PageRank to learn weights for k -hop neighbor aggregations. HOG-GCN [18] constructs a homophily degree matrix with attribute and topological information to adaptively modify the feature propagation process. To enhance the computational efficiency on large-scale graphs, LINKX [12] considers the adjacency matrix as an additional channel of node features. CPGNN [27] learns a compatibility matrix by modeling the prior beliefs of the nodes. LFL [22] designs an adaptive filter initialized with link prediction under the weakly-supervised settings.

The neighbor extension methods focus on constructing new filters or new graph structures to extend neighbors to global nodes. To adaptively integrate different signals during the message aggregation, FAGCN [2] incorporates both the low and high-frequency filters in GCNs. Based on this approach, ACM-GCN [13] further employs low-pass, high-pass, and identity channels to adaptively mix different levels of frequency signals. To preserve topological information and capture long-range dependencies, Geom-GNN [14] constructs structural neighbors using geometric measurements. To address both the over-smoothing and heterophily problems, GGCN [23] corrects original edges by considering node structures or features. To extend neighbors to nodes with similar semantics, WRGAT [16] learns a new computation graph based on proximity and local structural similarity of nodes. To aggregate the information from global nodes in graphs, GloGNN [11] learns a coefficient matrix to capture the correlations between nodes by considering both feature similarity and topology similarity. L2A [20] performs graph structure augmentation into a continuous optimization problem with a variational inference approach.

The aggregation calibration methods perform message passing from a local perspective, thereby failing to capture long-range dependencies from global nodes. To address the issue, current neighbor extension methods establish new connections with global nodes by utilizing either feature information, node structural information, or new filters. However, these methods overlook heterophilous information, which describes the contexts of homophilous or heterophilous nodes. This heterophilous information provides rich semantics of a node that cannot be obtained through node features or topological information.

6 Conclusion

This paper introduces the concept of heterophilous information as the distribution of node neighbors and proposes a practical solution to effectively leverage the rich semantics present in graphs. The new graph structure in our proposed HiGNN improves the connectivity between nodes with identical labels, thereby accommodating datasets with varying homophily, as shown by our theoretical and empirical analysis. Our experiments show the superiority of HiGNN in handling both homophilous and heterophilous graphs. It is worth noting that while HiGNN enhances the graph learning, it depends on the prior estimation of all node labels. This dependency not only hinges on the quality of label estimation but also increases computational complexity. In our future work, we aim to explore more efficient representations of heterophilous information that strike a balance between computational demands and performance.

A Proof of Theorem 1

Theorem 2. *The homophily degree \hat{h} of A' is directly proportional to the threshold δ , inversely proportional to the variance σ^2 of sampling noise, and directly proportional to the distance between the original homophily degree and reciprocal of c :*

$$\hat{h} \propto \delta, \hat{h} \propto \frac{1}{\sigma^2}, \hat{h} \propto |h - \frac{1}{c}| \quad (10)$$

Proof. We first make the following assumptions:

- Every node has a probability of h to connect with intra-class nodes, and a probability of $\frac{1-h}{c-1}$ to connect with inter-class nodes. Each probability is corrupted by an independent Gaussian noise $\epsilon \sim N(0, \sigma^2)$.
- The number of nodes is balanced across each class.

Following the assumptions, we ensure the original homophily degree is h . Besides, we can get the heterophilous information of node u as

$$\mathcal{H}_u = [p_1, p_2, \dots, p_c], \text{ where } p_i = \begin{cases} h + \epsilon_{u,i} & \text{if } i = y_u \\ \frac{1-h}{c-1} + \epsilon_{u,i} & \text{if } i \neq y_u \end{cases} \quad (11)$$

Then we define the similarity of the neighbor distribution of node u and v as \mathcal{S}^+ when $y_u = y_v$, and \mathcal{S}^- when $y_u \neq y_v$. Then we have

$$\begin{aligned}
\mathbf{S}^+ &= \cos(\mathcal{H}_u, \mathcal{H}_v) \\
&= \frac{1}{\mathcal{H}_{norm}} \left((h + \epsilon_{v,y_v})(h + \epsilon_{u,y_u}) + \sum_{\substack{i=1, \\ i \neq y_u}}^c \left(\frac{1-h}{c-1} + \epsilon_{u,i} \right) \left(\frac{1-h}{c-1} + \epsilon_{v,i} \right) \right) \\
\mathbf{S}^- &= \cos(\mathcal{H}_u, \mathcal{H}_v) \\
&= \frac{1}{\mathcal{H}_{norm}} \left((h + \epsilon_{u,y_u}) \left(\frac{1-h}{c-1} + \epsilon_{v,y_v} \right) + (h + \epsilon_{v,y_v}) \left(\frac{1-h}{c-1} + \epsilon_{u,y_u} \right) \right. \\
&\quad \left. + \sum_{\substack{i=1, \\ i \neq y_u, i \neq y_v}}^c \left(\frac{1-h}{c-1} + \epsilon_{u,i} \right) \left(\frac{1-h}{c-1} + \epsilon_{v,i} \right) \right)
\end{aligned} \tag{12}$$

where $\mathcal{H}_{norm} = \|\mathcal{H}_u\| \|\mathcal{H}_v\|$.

The new homophily degree \hat{h} of the newly constructed A' can be expressed as the ratio of homophilous edges to the total number of edges

$$\hat{h} = \frac{P(\mathbf{S}^+ > \delta)}{P(\mathbf{S}^+ > \delta) + (c-1)P(\mathbf{S}^- > \delta)} \tag{13}$$

To simplify the analysis, we ignore the second order of noise term $\epsilon_{u,i}\epsilon_{v,i}$ since its magnitude is much smaller than the other terms. We also treat the normalization term \mathcal{H}_{norm} as a constant, by omitting the noise term, as \mathcal{H}_{norm} is identical for both the \mathbf{S}^+ and \mathbf{S}^- . Consequently, we can express \mathbf{S}^+ as

$$\mathbf{S}^+ = \mathcal{H}_{norm}^{-1} \left(h^2 + \frac{(1-h)^2}{c-1} + \epsilon^+ \right) \tag{14}$$

where $\epsilon^+ = h(\epsilon_{u,y_u} + \epsilon_{v,y_v}) + \sum_{i=1, i \neq y_u}^c \frac{1-h}{c-1} (\epsilon_{u,i} + \epsilon_{v,i}) \sim N(0, (h^2 + \frac{(1-h)^2}{c-1})2\sigma^2)$.

Then we can get the probability of homophilous edges as

$$\begin{aligned}
P(\mathbf{S}^+ > \delta) &= P\left(\left(\mathcal{H}_{norm}^{-1} \left(h^2 + \frac{(1-h)^2}{c-1} + \epsilon^+ \right)\right) > \delta\right) \\
&= P\left(\epsilon^+ > \delta\mathcal{H}_{norm} - h^2 - \frac{(1-h)^2}{c-1}\right) \\
&= \Phi\left(\frac{h^2 + \frac{(1-h)^2}{c-1} - \delta\mathcal{H}_{norm}}{(h^2 + \frac{(1-h)^2}{c-1})^{\frac{1}{2}}\sqrt{2}\sigma}\right)
\end{aligned} \tag{15}$$

Let $t_+ = \frac{h^2 + \frac{(1-h)^2}{c-1} - \delta\mathcal{H}_{norm}}{(h^2 + \frac{(1-h)^2}{c-1})^{\frac{1}{2}}\sqrt{2}\sigma}$, we have $P(\mathbf{S}^+ > \delta) = \Phi(t_+)$.

Similarly, for \mathbf{S}^- , we follow the same process as \mathbf{S}^+ and we can get $P(\mathbf{S}^- > \delta) = \Phi(t_-)$, where $t_- = \frac{2h\frac{1-h}{c-1} + (C-2)(\frac{1-h}{c-1})^2 - \delta\mathcal{H}_{norm}}{(h^2 + \frac{(1-h)^2}{c-1})^{\frac{1}{2}}\sqrt{2}\sigma}$.

Next, we substitute $P(\mathbf{S}^+ > \delta)$ and $P(\mathbf{S}^- > \delta)$ into Eq. 13 to get the new homophily degree

$$\hat{h} = \left(1 + (c-1) \frac{\Phi(t_-)}{\Phi(t_+)}\right)^{-1} \quad (16)$$

We then analyze the influence of the threshold δ , the standard variance of noise σ , and the original homophily degree h by taking partial derivative with respect to \hat{h}

$$\frac{\partial \hat{h}}{\partial \delta} \geq 0, \quad \frac{\partial \hat{h}}{\partial \sigma} \leq 0, \quad \frac{\partial \hat{h}}{\partial h} \begin{cases} \geq 0 & \text{if } h \geq \frac{1}{c} \\ < 0 & \text{if } h < \frac{1}{c} \end{cases} \quad (17)$$

From the partial derivative results, we can get Theorem 2 proved.

References

1. Abu-El-Haija, S., Perozzi, B., Kapoor, A., Alipourfard, N., Lerman, K., Harutyunyan, H., Ver Steeg, G., Galstyan, A.: Mixhop: Higher-order graph convolutional architectures via sparsified neighborhood mixing. In: international conference on machine learning. pp. 21–29. PMLR (2019)
2. Bo, D., Wang, X., Shi, C., Shen, H.: Beyond low-frequency information in graph convolutional networks. In: Proceedings of the AAAI Conference on Artificial Intelligence. vol. 35, pp. 3950–3957 (2021)
3. Chen, M., Wei, Z., Huang, Z., Ding, B., Li, Y.: Simple and deep graph convolutional networks. In: International conference on machine learning. pp. 1725–1735. PMLR (2020)
4. Chien, E., Peng, J., Li, P., Milenkovic, O.: Adaptive universal generalized pagerank graph neural network. arXiv preprint arXiv:2006.07988 (2020)
5. Duvenaud, D., Maclaurin, D., Aguilera-Iparraguirre, J., Gómez-Bombarelli, R., Hirzel, T., Aspuru-Guzik, A., Adams, R.P.: Convolutional networks on graphs for learning molecular fingerprints. In: Cortes, C., Lawrence, N.D., Lee, D.D., Sugiyama, M., Garnett, R. (eds.) Advances in Neural Information Processing Systems 28: Annual Conference on Neural Information Processing Systems 2015, December 7–12, 2015, Montreal, Quebec, Canada. pp. 2224–2232 (2015)
6. Guo, J., Du, L., Bi, W., Fu, Q., Ma, X., Chen, X., Han, S., Zhang, D., Zhang, Y.: Homophily-oriented heterogeneous graph rewiring. In: Proceedings of the ACM Web Conference 2023. p. 511–522. WWW ’23, Association for Computing Machinery, New York, NY, USA (2023)
7. Guo, K., Cao, X., Liu, Z., Chang, Y.: Taming over-smoothing representation on heterophilic graphs. Information Sciences **647**, 119463 (2023)
8. Guo, Z., Wang, H.: A deep graph neural network-based mechanism for social recommendations. IEEE Transactions on Industrial Informatics **17**(4), 2776–2783 (2021)
9. Hamilton, W.L., Ying, Z., Leskovec, J.: Inductive representation learning on large graphs. In: Guyon, I., von Luxburg, U., Bengio, S., Wallach, H.M., Fergus, R., Vishwanathan, S.V.N., Garnett, R. (eds.) Advances in Neural Information Processing Systems 30: Annual Conference on Neural Information Processing Systems 2017, December 4–9, 2017, Long Beach, CA, USA. pp. 1024–1034 (2017)

10. Kipf, T.N., Welling, M.: Semi-supervised classification with graph convolutional networks. arXiv preprint arXiv:1609.02907 (2016)
11. Li, X., Zhu, R., Cheng, Y., Shan, C., Luo, S., Li, D., Qian, W.: Finding global homophily in graph neural networks when meeting heterophily. In: International Conference on Machine Learning. pp. 13242–13256. PMLR (2022)
12. Lim, D., Hohne, F., Li, X., Huang, S.L., Gupta, V., Bhalerao, O., Lim, S.N.: Large scale learning on non-homophilous graphs: New benchmarks and strong simple methods. *Advances in Neural Information Processing Systems* **34**, 20887–20902 (2021)
13. Luan, S., Hua, C., Lu, Q., Zhu, J., Zhao, M., Zhang, S., Chang, X.W., Precup, D.: Is heterophily a real nightmare for graph neural networks to do node classification? arXiv preprint arXiv:2109.05641 (2021)
14. Pei, H., Wei, B., Chang, K.C., Lei, Y., Yang, B.: Geom-gcn: Geometric graph convolutional networks. In: 8th International Conference on Learning Representations, ICLR 2020, Addis Ababa, Ethiopia, April 26–30, 2020. OpenReview.net (2020)
15. Pei, H., Wei, B., Chang, K.C., Lei, Y., Yang, B.: Geom-gcn: Geometric graph convolutional networks. In: 8th International Conference on Learning Representations, ICLR 2020, Addis Ababa, Ethiopia, April 26–30, 2020. OpenReview.net (2020)
16. Suresh, S., Budde, V., Neville, J., Li, P., Ma, J.: Breaking the limit of graph neural networks by improving the assortativity of graphs with local mixing patterns. In: Proceedings of the 27th ACM SIGKDD Conference on Knowledge Discovery & Data Mining. pp. 1541–1551 (2021)
17. Velickovic, P., Cucurull, G., Casanova, A., Romero, A., Lio, P., Bengio, Y., et al.: Graph attention networks. *stat* **1050**(20), 10–48550 (2017)
18. Wang, T., Wang, R., Jin, D., He, D., Huang, Y.: Powerful graph convolutional networks with adaptive propagation mechanism for homophily and heterophily. *CoRR* **abs/2112.13562** (2021)
19. Wu, F., Souza, A., Zhang, T., Fifty, C., Yu, T., Weinberger, K.: Simplifying graph convolutional networks. In: International conference on machine learning. pp. 6861–6871. PMLR (2019)
20. Wu, L., Tan, C., Liu, Z., Gao, Z., Lin, H., Li, S.Z.: Learning to augment graph structure for both homophily and heterophily graphs. In: Koutra, D., Plant, C., Gomez Rodriguez, M., Baralis, E., Bonchi, F. (eds.) *Machine Learning and Knowledge Discovery in Databases: Research Track*. pp. 3–18. Springer Nature Switzerland, Cham (2023)
21. Wu, S., Tang, Y., Zhu, Y., Wang, L., Xie, X., Tan, T.: Session-based recommendation with graph neural networks. *Proceedings of the AAAI Conference on Artificial Intelligence* **33**(01), 346–353 (Jul 2019)
22. Wu, X., Wu, H., Wang, R., Li, D., Zhou, X., Lu, K.: Leveraging free labels to power up heterophilic graph learning in weakly-supervised settings: An empirical study. In: Koutra, D., Plant, C., Gomez Rodriguez, M., Baralis, E., Bonchi, F. (eds.) *Machine Learning and Knowledge Discovery in Databases: Research Track*. pp. 140–156. Springer Nature Switzerland, Cham (2023)
23. Yan, Y., Hashemi, M., Swersky, K., Yang, Y., Koutra, D.: Two sides of the same coin: Heterophily and oversmoothing in graph convolutional neural networks. In: 2022 IEEE International Conference on Data Mining (ICDM). pp. 1287–1292. IEEE (2022)
24. Zhang, K., Wang, W., Zhang, H., Li, G., Jin, Z.: Learning to represent programs with heterogeneous graphs. In: Rastogi, A., Tufano, R., Bavota, G., Arnaoudova, V., Haiduc, S. (eds.) *Proceedings of the 30th IEEE/ACM International Conference*

- on Program Comprehension, ICPC 2022, Virtual Event, May 16-17, 2022. pp. 378–389. ACM (2022)
25. Zheng, X., Liu, Y., Pan, S., Zhang, M., Jin, D., Yu, P.S.: Graph neural networks for graphs with heterophily: A survey. CoRR **abs/2202.07082** (2022)
26. Zhu, J., Jin, J., Loveland, D., Schaub, M.T., Koutra, D.: How does heterophily impact the robustness of graph neural networks?: Theoretical connections and practical implications. In: Zhang, A., Rangwala, H. (eds.) KDD '22: The 28th ACM SIGKDD Conference on Knowledge Discovery and Data Mining, Washington, DC, USA, August 14 - 18, 2022. pp. 2637–2647. ACM (2022)
27. Zhu, J., Rossi, R.A., Rao, A., Mai, T., Lipka, N., Ahmed, N.K., Koutra, D.: Graph neural networks with heterophily. In: Thirty-Fifth AAAI Conference on Artificial Intelligence, AAAI 2021, Thirty-Third Conference on Innovative Applications of Artificial Intelligence, IAAI 2021, The Eleventh Symposium on Educational Advances in Artificial Intelligence, EAAI 2021, Virtual Event, February 2-9, 2021. pp. 11168–11176. AAAI Press (2021)
28. Zhu, J., Yan, Y., Zhao, L., Heimann, M., Akoglu, L., Koutra, D.: Beyond homophily in graph neural networks: Current limitations and effective designs. *Advances in neural information processing systems* **33**, 7793–7804 (2020)